Preferred citation: E.U. Schlünder. Through-drying of textiles and paper. In **Fibre-Water Interactions in Paper-Making**, *Trans. of the VIth Fund. Res. Symp. Oxford, 1977*, (Fundamental Research Committee, ed.), pp 443–455, FRC, Manchester, 2018. DOI: 10.15376/frc.1977.1.443.

THROUGH-DRYING OF TEXTILES AND PAPER

E. U. SCHLÜNDER, Institut für Thermische Verfahrenstechnik, Universität Karlsruhe, Germany

Synopsis Special laboratory equipment has been developed to measure drying rates as a function of the product moisture content for Through-Drying of textiles, porous paper and other permeable products. This equipment allows very precise measurements even for very fast drying processes (1 second and less), which are typical in Through-Drying. Experimental results for the drying rate as well as for the permeability (pressure drop) as a function of the product moisture content for various drying conditions for porous paper (tissue) are presented. The analysis of these results reveals, that the drying rate during the 'constant rate period' (surface evaporation period) can be predicted from standard heat and mass transfer equations only if the pore size distribution is taken into account. For the purpose of extrapolation and scale-up a special overall mass transfer equation has been introduced. For Through-Drying of tissue material, and of textiles, this equation represents the experimental results with fairly good accuracy.

Introduction

THROUGH-DRYING can be used for sufficiently permeable products, e.g. textiles, porous paper, tissue etc. Its advantages are short drying times, high saturation of the drying agent with water vapour, thus lowering energy consumption and sometimes improvement of the product quality.

For Through-Dryer design, information for the prediction of the residence time required to remove a certain amount of water from the product must be available.

This information can be obtained from the so-called drying rate diagram, which represents the drying rate $\mathrm{d}Y/\mathrm{d}t$ as a function of the product moisture content Y for constant drying conditions.

In the past many attempts have been made to predict drying rate diagrams from some fundamental physical properties of the product. Today these attempts have been given up, since the experimental determination of a whole drying rate diagram is much faster and cheaper, than the determination of

Under the chairmanship of Dr J. D. Peel the physical properties, not mentioning the enormous difficulties arising with the set up of a respective theory for the prediction of drying rate diagrams based on these physical properties.

Therefore, it is necessary to develop standard laboratory equipment for the experimental determination of drying rate diagrams. Also, it is necessary to develop, in parallel, suitable physical models or rules in order to extrapolate drying rate diagrams for other drying conditions, thus reducing the number of standard laboratory experiments. This has been done during the investigation for the Through-Drying process as reported here.

Experiments

THROUGH-DRYING of tissue material with hot air may be very fast, e.g. a few seconds and less. Moreover, the pressure drop at the moist sample varies considerably with the moisture content, which means that the flow rate of the drying agent varies with the moisture content of the product, too.

Therefore, the drying rate was determined by measuring the moisture content of the sample by an infrared absorption moisture meter. This method allows a direct and continuous recording of the drying rate without any disturbance or interruption of the drying process itself.

In order to establish unique and reproducible drying conditions the air supply was equipped with a supersonic nozzle in order to guarantee a constant

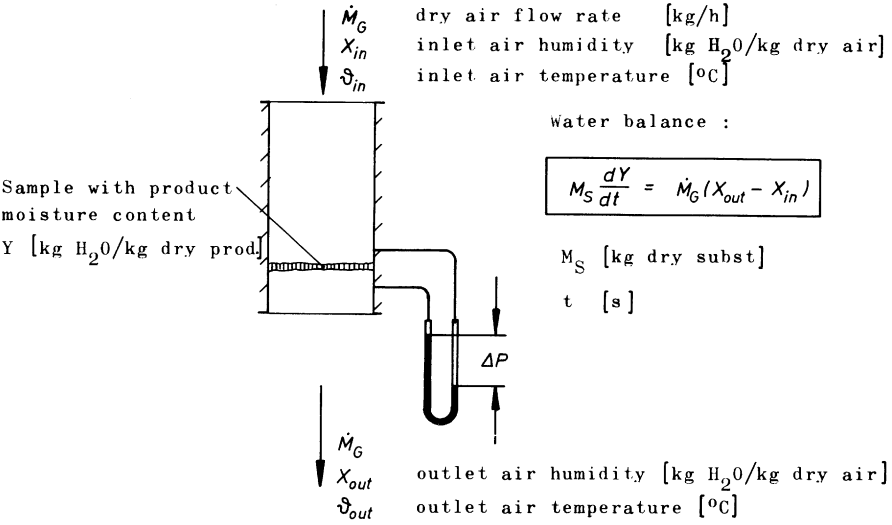

Fig. 1—Experimental method (schematic)

air flow rate regardless of the varying pressure drop at the sample with decreasing product moisture content.

The experimental method is shown schematically in Fig. 1 and in detail in Fig. 2.

The moisture meter 14 has been described in detail elsewhere.(1) An original plot of the outlet air humidity X_{out}, the outlet air temperature ϑ_{out} and the pressure drop through the sample Δp shows the variation of these quantities with the drying time, Fig. 3. The sample was a woollen textile with 1·25 kg H_2O/kg dry substance initial moisture content and 204 g dry subst./m^2 grammage. For porous paper, tissue, etc. one obtains the same type of curves.

From this original plot one obtains the moisture content of the sample as a function of the drying time by integration of the instantaneous water balance:

$$-M_S\frac{\mathrm{d}Y}{\mathrm{d}t} = \dot{M}_G(X_{\text{out}}(t)-X_{\text{in}}). \quad . \quad . \quad . \quad (1)$$

The total weight of the sample was determined before and after each run. For sufficiently long drying time ($t \to \infty$) the product moisture content tends towards the hygroscopic equilibrium moisture content Y_{hygr}. With these

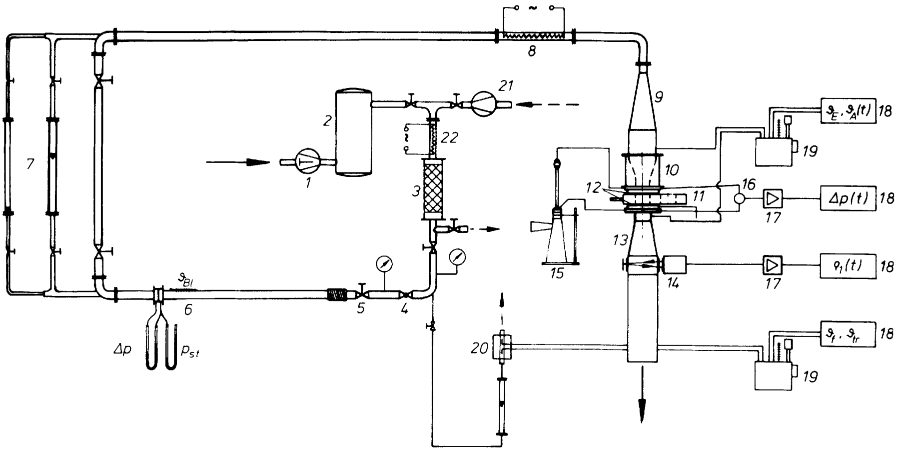

Fig. 2—Experimental method in detail

1 compressor
2 pressure vessel
3 molecular sieve
4 supersonic nozzle
5 control valve
6 flow meter
7 rotameter
8 heating
9 diffuse
10 nozzle
11 sample holder
12 gasket
13 adapter
14 moisture meter
15 Betz manometer
16 pressure transducer
17 amplifier
18 recorders
19 thermostat
20 psychrometer
21 ventilator } for regenerating the
22 heater } molecular sieve

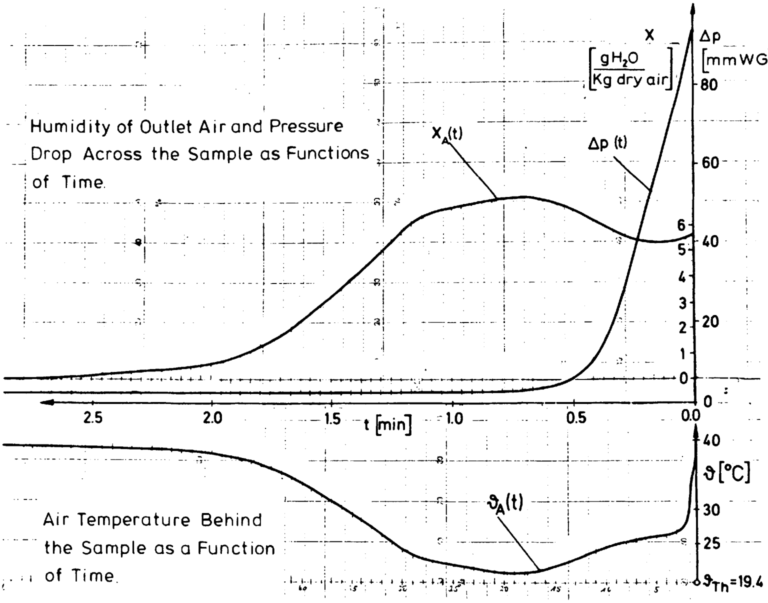

Fig. 3 —Original recording of outlet air humidity X_{out}, outlet air temperature ϑ_{out} and pressure drop Δp against the drying time t, for a woollen textile with initial moisture content $Y_0 = 1{\cdot}25$ kg H_2O/kg dry subst. The air flow rate was $\dot{M}_G/f = 0{\cdot}42$ kg dry air/m^{2}s

limits the integration of equation (*1*) yields:

$$\frac{Y_0 - Y(t)}{Y_0 - Y_{\text{hygr}}} = \frac{\int_0 (X_{\text{out}}(t) - X_{\text{in}})\,dt}{\int_0^{t\to\infty} (X_{\text{out}}(t) - X_{\text{in}})\,dt} \quad . \quad . \quad . \quad . \qquad (2)$$

With all the runs the inlet air humidity X_{in} has been practically zero (dew point −70° C) and therefore also Y_{hygr} was close to zero.

Fig. 4 shows the drying rate determined by equation (*1*) plotted against the product moisture content determined by equation (*2*) for a tissue sample at various air flow rates and various air inlet temperatures. Also, the pressure drop depending on the product moisture content is shown in this figure. About 400 runs for tissue as well as for various textiles have been reported in 'Durchströmungstrocknung', Dissertation Universität Karlsruhe, 1977, by P. Gummel.(2)

The results of these are summarised in the following.

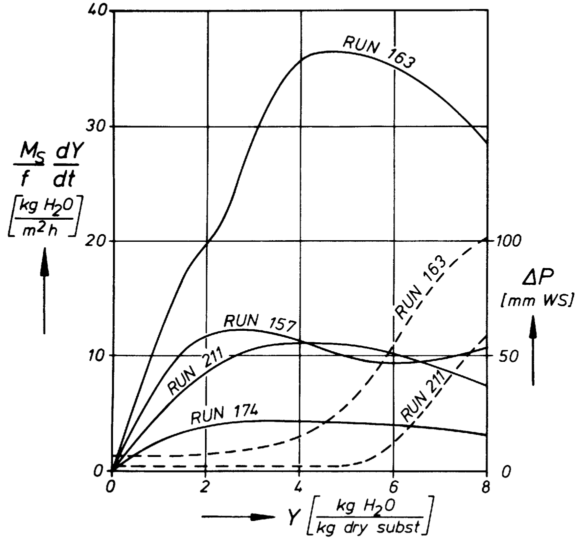

RUN	$\dot{M}_G/f$ $\left[\frac{kg\ dry\ air}{m^2 s}\right]$	ϑ_{in} [°C]	X_{in} $\left[\frac{g\ H_2O}{kg\ dry\ air}\right]$
163	0,80	94,9	0,00
211	0,20	87,2	0,61
157	0,81	24,0	0,00
174	0,21	22,0	0,04

Fig. 4—Drying rate a pressure drop as functions of the product moisture content for tissue material at various air temperatures

General

(*1*) The pressure drop Δp decreases rapidly with decreasing moisture content of the sample and reaches its minimum value, which is the same as for the dry sample, when the outlet air humidity X_{out}, and, therefore, the drying rate $\mathrm{d}Y/\mathrm{d}t$ (see Fig. 1), reach their maximum values. At the same point the outlet air temperature ϑ_{out} comes close to the wet bulb temperature ϑ_{WB}.

(*2*) No constant drying rate period in the rigorous sense of the word has been observed, but there was always a maximum drying rate at a still relatively high moisture content of the sample coincidence with the minimum pressure drop.

(*3*) During the falling rate period, mainly *free* water is removed. The maximum *adsorbed* moisture content of tissue paper is about 0·2 to 0·3 kg H_2O/kg dry substance (Fig. 5).

Pressure drop through the dry sample

FIG. 6 shows the pressure drop through two different dry tissue samples, Nos. 11 and 12.

Two flow regimes can be recognised in Fig. 6. There is the fully developed laminar flow regime for $W_0/v < 20\,000$/m, where the pressure drop is proportional to the air velocity ($\Delta p \sim W_0$) and the nondeveloped laminar flow regime, where Δp is proportional to the 1·5th power of W_0 ($\Delta p \sim W_0^{1\cdot5}$).

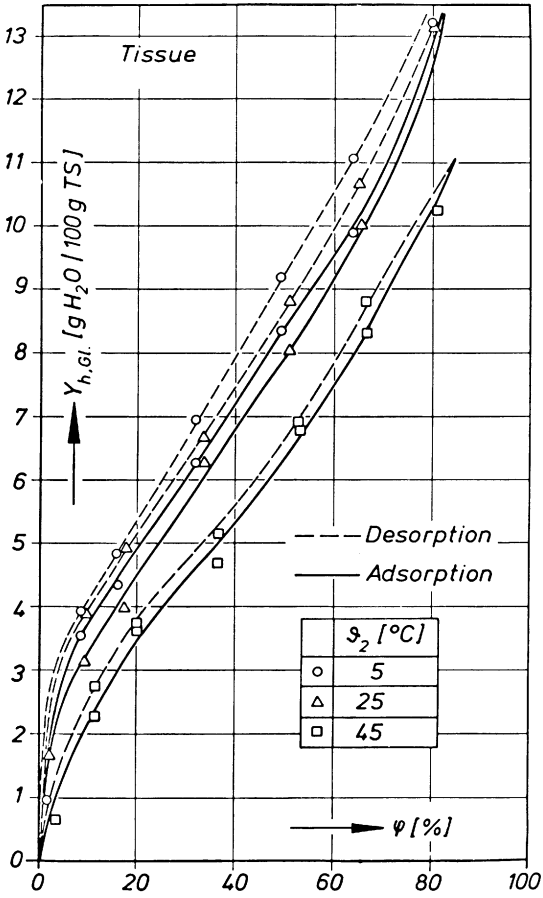

Fig. 5—Sorption isotherms for tissue samples

Applying the Hagen–Poiseuille law in the fully developed laminar flow regime one can derive an equivalent average pore diameter

$$d_{eq} = \sqrt{\frac{128\eta L W_0}{\psi\, \Delta P}}, \qquad (3)$$

where

$$W_0 = \dot{M}_G / \rho_G f. \qquad (4)$$

ψ is the void fraction of the sample cross section, L the thickness of the sample and η the air viscosity. For the tissue sample 11 one obtains from the $\Delta p - W_0$-plot, $d_{eq} = 169$ μm with $\psi = 15$ per cent, $L = 257$ μm and for tissue sample

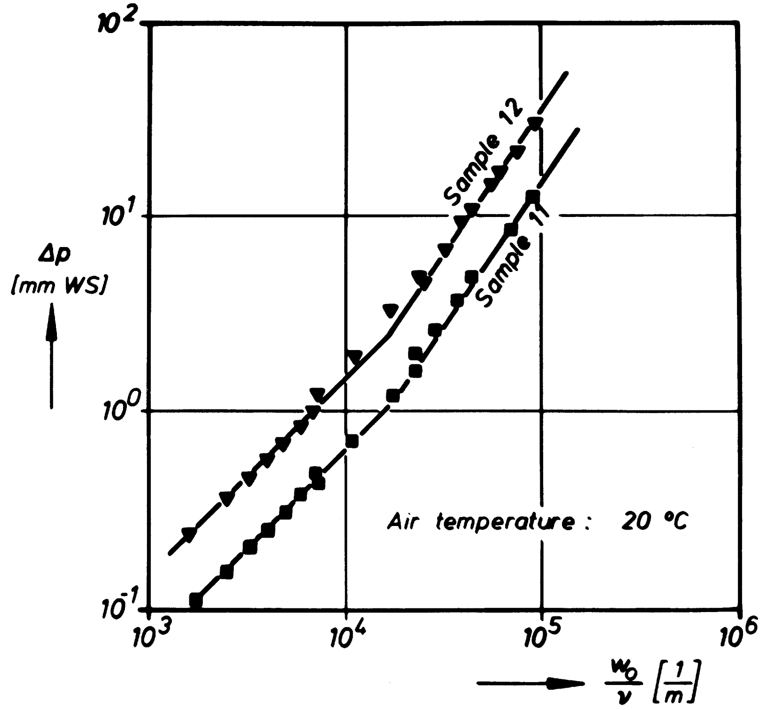

Fig. 6—Pressure drop through dry tissue

12 the data are $d_{eq} = 129$ μm with $\psi = 10$ per cent, $L = 258$ μm. The order of magnitude of d_{eq}, ψ and L are in fairly good agreement with microscopic observations (Fig. 7).

With these quantities, d_{eq}, ψ and L, the pressure drop in the nondeveloped laminar flow regime can be predicted, applying the tube flow formula

$$\Delta p = 13{\cdot}8 \cdot \sqrt{\frac{\nu L}{d_{eq}{}^2} \frac{\rho}{2}} \left(\frac{W_0}{\psi}\right)^{1{\cdot}5} \quad . \quad . \quad . \quad . \quad . \quad (5)$$

Mass transfer between air and sample surface

CONSIDERING the tissue sample as a bundle of equal sized capillaries having diameter d_{eq} and length L, the mass transfer between the air and the walls of these capillaries should be predictable applying the well known formula for the prediction of mass transfer coefficients in laminar tube flow. For a

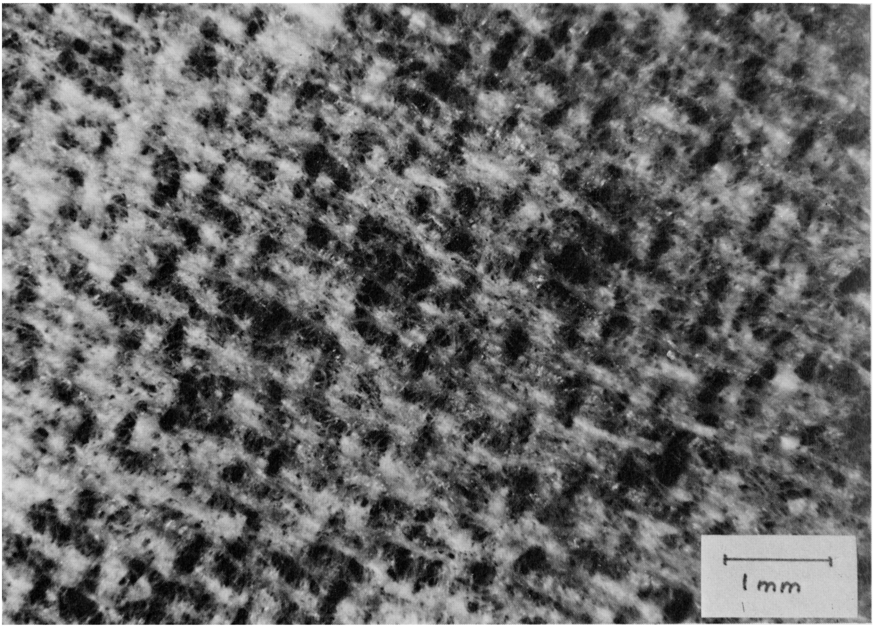

Fig. 7—Tissue, sample 11

Schmidt number of $Sc = 0{\cdot}57$, which applies to the air/H_2O system this formula reads

$$Sh = \sqrt[3]{49 + \left(4{\cdot}2 + 0{\cdot}388\sqrt{\mathrm{Pe}\,\frac{d_{\mathrm{eq}}}{L}}\right)^{1} \mathrm{Pe}\,\frac{d_{\mathrm{eq}}}{L}}. \qquad (6)$$

It covers the fully developed as well as the nondeveloped laminar flow regime. In this equation we have

$$\mathrm{Sh} = \beta d_{\mathrm{eq}}/\delta \qquad \text{and} \qquad \mathrm{Pe} = W_0 d_{\mathrm{eq}}/\delta,$$

where δ is the diffusivity of H_2O vapour in air. The number of transfer units (NTU) is given by

$$\mathrm{NTU} = \beta A/\dot{V}_G, \qquad (7)$$

where A is the surface area of the capillary, and is connected with Sh and Pe d_{eq}/L by the definition:

$$\mathrm{Sh} = \tfrac{1}{4}\mathrm{NTU}\cdot\mathrm{Pe}\,d_{\mathrm{eq}}/L. \qquad (8)$$

The NTU can be determined directly from the experimental data

$$\mathrm{NTU} = \ln\frac{X^* - X_{\mathrm{in}}}{X^* - X_{\mathrm{out}}} \qquad (9)$$

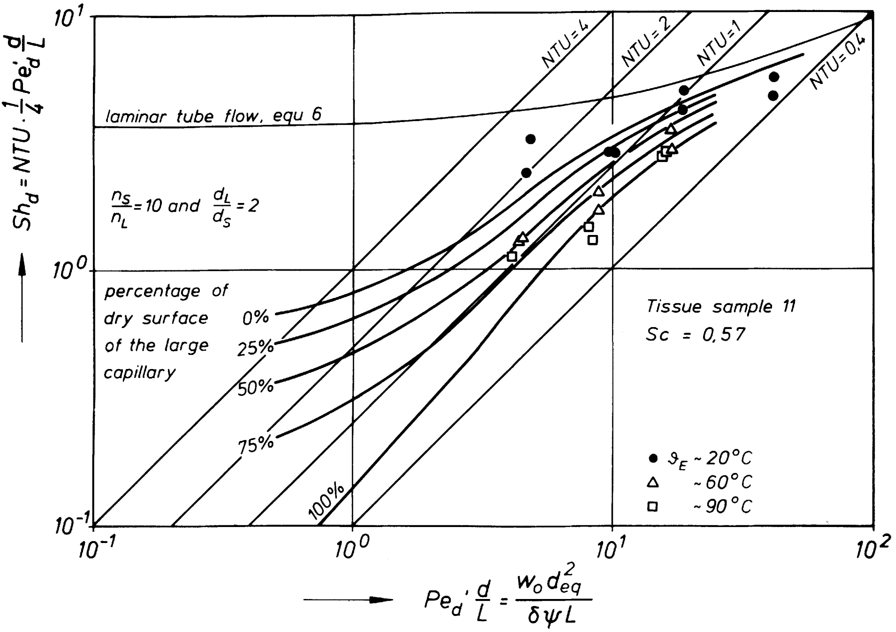

Fig. 8—Mass transfer between air and tissue, sample 11
n_S = number of small capillaries
n_L = number of large capillaries

where X^* is the saturation air humidity at the wet bulb temperature corresponding to ϑ_{in} and X_{in}. Equation (*9*) implies that there is no axial dispersion in the air flow. Assuming that the sample is at the wet bulb temperature when the outlet air humidity X_{out} reaches its maximum and the pressure drop its minimum value, as indicated by Fig. 3, one obtains the maximum NTU of each run

$$\mathrm{NTU}_{\max} = \ln \frac{X^* - X_{in}}{X^* - X_{out,\,max}} \quad . \quad . \quad . \quad . \quad . \qquad (10)$$

From these maximum NTU values, one can calculate the corresponding Sherwood numbers according to equation (*8*). These should coincide with the predicted Sherwood numbers according to equation (*6*). Obviously they do not as shown by the Figs. 8 and 9.

The experimental Sherwood numbers are considerably lower than the predicted ones for a bundle of equal-sized capillaries. The deviations are larger when the air inlet temperature is high. On the other hand, they are also

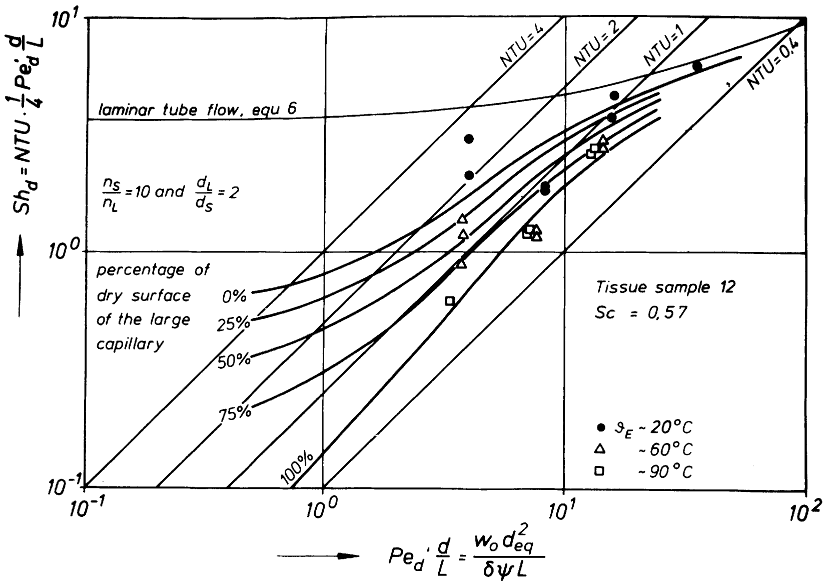

Fig. 9—Mass transfer between air and tissue, sample 12
n_S = number of small capillaries
n_L = number of large capillaries

larger when the air velocity is low. These deviations may have been caused by

(*1*) axial dispersion of the air flow;
(*2*) non-uniform size distribution of the capillaries;
(*3*) no pure surface evaporation at the maximum drying rate.

Axial dispersion, though it may have a small effect, was neglected. On the other hand it is evident, that a certain size distribution of the capillary diameter will lower the average Sherwood number considerably. The curves in Figs. 8 and 9, marked with the parameter 0 per cent, follow directly from equation (*6*), when it is assumed, that 10 per cent of all the capillaries have twice the diameter of all the others ($n_S/n_L = 10$). The parameter 0 per cent means, that the large capillaries are also entirely wet. The parameter 100 per cent means, that the large capillaries are entirely dry, while the small ones are still wet. The theory for the prediction of these curves has been given elsewhere.(2, 3)

The Figs. 8 and 9 show that at low air temperature (20° C) the deviations can be explained by a capillary size distribution only. The small as well as the large capillaries are entirely wet (0 per cent dry). For large air temperatures

(90° C), however, one must assume that the large capillaries are completely dry, when the drying rate has reached its maximum value (100 per cent dry). This does not seem to be unrealistic, since the mass transfer rates in the large capillaries are considerably higher than in the small ones.

Normalised drying rate diagrams

SINCE the air humidity increases while the air passes through the sample, the local drying conditions within the sample are not constant. Therefore the experimental drying rates must be related to a constant reference state of the drying agent. This reference state should be the inlet conditions of the air $(\vartheta_{\text{in}}, X_{\text{in}})$.

Before reducing the experimental data to this reference state, three assumptions have to be made. Firstly, it is assumed that there is no axial dispersion of the air humidity and, secondly, it is assumed, that there is perfect axial dispersion of the product moisture content. The latter assumption means that there are no Y-profiles in the flow direction of the drying agent. Thirdly, it is assumed that the drying rate may be expressed as a product of two functions, one depending on the air humidity X and the other one on the product moisture content Y.

For X, the reference air humidity is taken to be the wet bulb saturation humidity $X = X^* (\vartheta_{\text{in}}, X_{\text{in}})$. For Y, the reference product moisture content may be Y_{crit}, which is the value where the maximum drying rate appears. Thus we introduce a dimensionless air humidity

$$\xi = \frac{X^* - X}{X^* - X_{\text{in}}} \quad . \quad . \quad . \quad . \quad . \quad . \quad (11)$$

and a dimensionless product moisture content

$$\eta = \frac{Y - Y_{\text{hygr}}}{Y_{\text{crit}} - Y_{\text{hygr}}}. \quad . \quad . \quad . \quad . \quad . \quad (12)$$

According to the third assumption, the local drying rate should be

$$-\mathrm{d}M_S \frac{\mathrm{d}Y}{\mathrm{d}t} = \rho_G \beta (X^* - X_{\text{in}}) \cdot \xi \cdot \dot{\nu}(\eta) \cdot \mathrm{d}A, \quad . \quad . \quad (13)$$

where $\dot{\nu}(\eta)$ is the normalised drying rate as a function of the dimensionless product moisture content. Substituting the left hand side in equation (*13*) with the local water balance

$$\mathrm{d}M_S \frac{\mathrm{d}Y}{\mathrm{d}t} + \dot{M}_G \, \mathrm{d}X = 0, \quad . \quad . \quad . \quad . \quad . \quad (14)$$

one obtains

$$-\frac{\mathrm{d}\xi}{\mathrm{d}\zeta} = \xi \cdot \dot{\nu}(\eta), \quad . \quad . \quad . \quad . \quad . \quad . \quad (15)$$

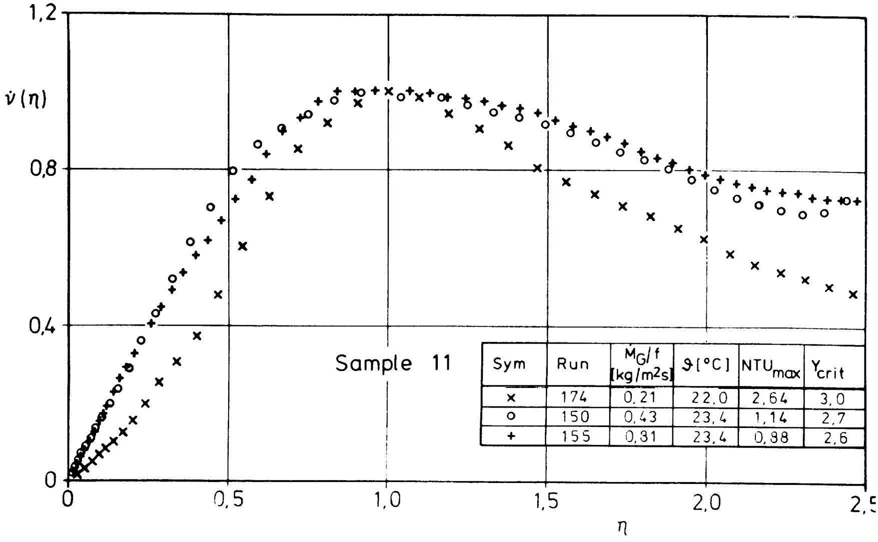

Fig. 10—Normalised drying rate as a function of the normalised product moisture content for tissue paper at various air flow rates and 23° C air temperature

where

$$d\zeta = \frac{\beta}{\dot V_G}\, dA. \quad . \quad . \quad . \quad . \quad . \quad . \qquad (16)$$

Integrating equation (*16*) from $\zeta = 0$ to $\zeta = \mathrm{NTU}_{\max}$ yields

$$\dot\nu(\eta) = \frac{\ln(X^* - X_{\mathrm{in}}/X^* - X_{\mathrm{out}})}{\mathrm{NTU}_{\max}} \qquad (17)$$

or

$$\dot\nu(\eta) = \frac{\ln(X^* - X_{\mathrm{in}}/X^* - X_{\mathrm{out}})}{\ln(X^* - X_{\mathrm{in}}/X^* - X_{\mathrm{out,\,max}})} \quad . \quad . \quad . \qquad (18)$$

By definition, $(\dot\nu\eta) = 1$, when $Y = Y_{\mathrm{crit}}$ or $\eta = 1$.

Figs. 10, 11 and 12 show some normalised drying rate diagrams for tissue, sample 11, calculated from equation (*18*). The result is, that for a certain air inlet temperature the function $\dot\nu(\eta)$ is nearly independent of the air flow rate $\dot M_G/f$ and therefore also independent of the air humidity ξ. This is important not only as justification of the empirical equation (*13*) but also for the purpose of extrapolation and for the application in dryer design and scale-up.

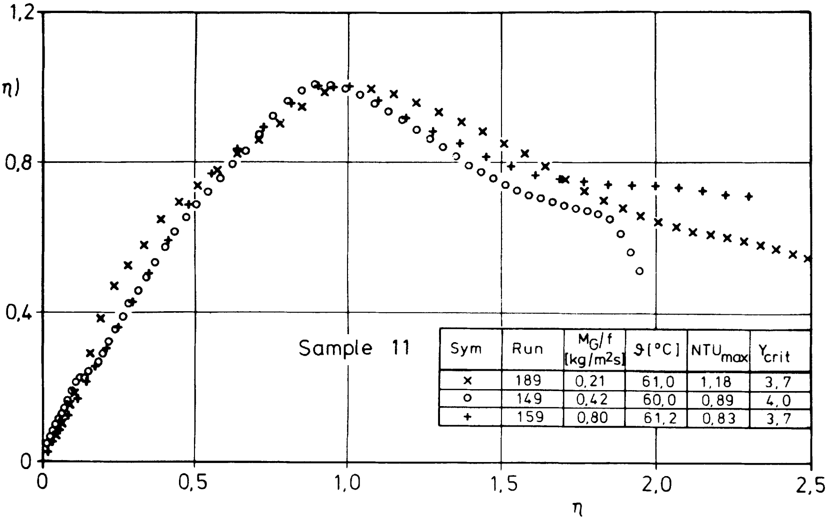

Sym	Run	M_G/f [kg/m²s]	ϑ[°C]	NTU_{max}	Y_{crit}
×	189	0,21	61,0	1,18	3,7
o	149	0,42	60,0	0,89	4,0
+	159	0,80	61,2	0,83	3,7

Fig. 11—As Fig. 10, but at 60° C air temperature

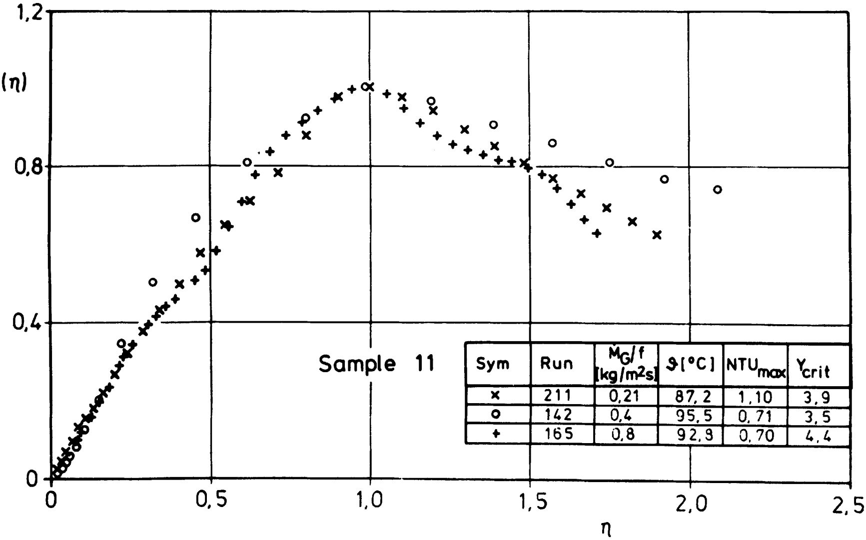

Sym	Run	M_G/f [kg/m²s]	ϑ[°C]	NTU_{max}	Y_{crit}
×	211	0,21	87,2	1,10	3,9
o	142	0,4	95,5	0,71	3,5
+	165	0,8	92,9	0,70	4,4

Fig. 12—As Fig. 10, but at 90° C air temperature

References

1. *Verfahrenstechnik*, 1976, **10** (12), 766
2. Gummel, P., Dissertation Karlsruhe University, 1977
3. Schlünder, E. U., *Verfahrenstechnik*, 1976, **10** (10), 645

Transcription of Discussion

Discussion

Dr A. M. Scallan I have some information which may act as confirmation of something that Prof. Schlünder has said. One thing that might not be as obvious to papermakers as it is to textile workers is that water goes from the large interfibre pores first and then leaves the individual fibres. Professor Schlünder's student gave a talk in Montreal and it led us to do a very simple experiment. We took some moist paper and suspended it from a recording balance inside a desiccated enclosure and monitored weight changes as a function of time. When we plotted the moisture content as grams water per gram solid against time we obtained a straight line indicating a steady loss of water, followed by a falling rate period. The moisture content at the end of the steady rate period corresponded to the fibre saturation point as determined separately by the solute exclusion technique. This would appear to confirm that the water leaves the interfibre pores first, and then the moist fibres from where it is more difficult to remove (Fig. 1).

Prof. B. K. Steenberg I believe that all of those here who are chemists and who have worked with sintered glass filters have observed that on suction one or two areas suddenly become opaque and these areas then start to increase in size. This is due to the largest capillaries emptying first. Then due to the flow they pull water from the surrounding area and the opaque areas get larger. This is exactly analogous except that the cause is not heat flow but fluid flow. The testing of the uniformity of glass filters in factories is based on this mechanism.

Schlünder Compared with through-drying, Dr Scallan's method is conducted at a low drying rate, lower by a factor of 10 or more, so there are differences. This is different to our experiments because capillary forces may compensate and equalise the moisture profiles in the fibres. Whether you have a pore size distribution formed by the fibres is irrelevant in this case.

Under the chairmanship of Dr J. D. Peel

Discussion

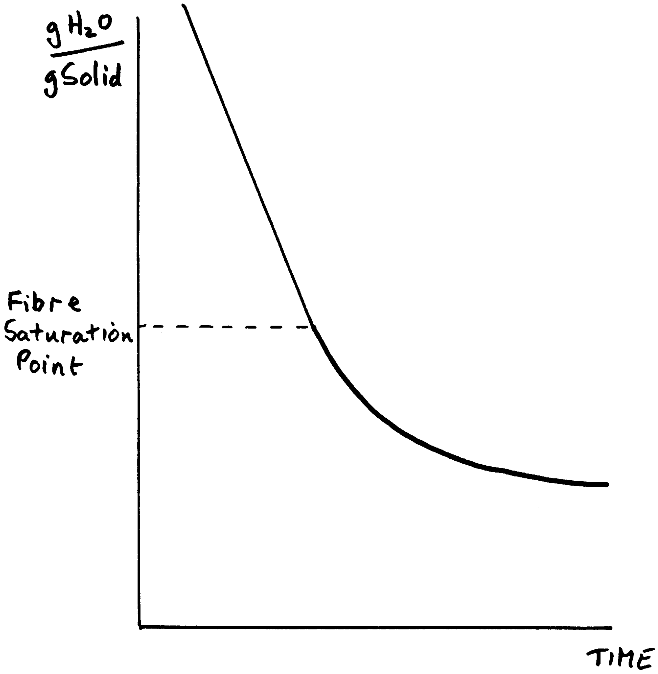

Fig. 1